Measuring the Wess-Zumino anomaly in τ decays

R. Decker and E. Mirkes
Institut für Theoretische Teilchenphysik, Universität Karlsruhe, Kaiserstrasse 12, Postfach 6980, 7500 Karlsruhe 1, Germany
(Received 28 December 1992)

We propose to measure the Wess-Zumino anomaly contribution by considering angular distributions in the decays $\tau\to\nu_\tau\eta\pi^-\pi^0$, $\tau\to\nu_\tau K^-\pi^-K^+$, and $\tau\to\nu_\tau K^-\pi^-\pi^+$. Radial excitations of the K^*, which cannot be seen in e^++e^-, should be observed in the $K^-\pi^+\pi^-$ decay channel.

PACS number(s): 13.35.+s, 11.40.Fy, 14.60.Jj

I. INTRODUCTION

With the experimental progress in τ decays, an ideal tool for studying strong-interaction physics has been developed. In this paper we show that several decays can be used to test the Wess-Zumino anomaly [1]. It appears that the anomaly violates the rule that the weak axial-vector and vector currents produce an odd and an even number of pseudoscalars, respectively. From its structure it can be seen that the anomaly contributes possibly to τ decays into $\nu_\tau+n$ mesons (with $n\geq 3$). Of course the golden-plated decay is $\tau\to\nu_\tau\eta\pi^-\pi^0$ which has a vanishing contribution from the axial-vector current [2–4]. Therefore a detected $\eta\pi^-\pi^0$ final state implies a nonvanishing anomaly. A recent measurement of its width [5] confirms the CVC (conserved vector current) predictions [3,4]. In this paper we will present the most general angular distribution of the $\eta\pi^-\pi^0$ system in terms of the vector current form factor for this channel. Furthermore, we demonstrate that also other decay modes in three pseudoscalars can be used to confirm (not only qualitatively) the presence of the Wess-Zumino anomaly. However, the most prominent decay channel into three pseudoscalars, i.e., $\pi^-\pi^-\pi^+$, cannot be used since G parity forbids the anomaly to contribute. Other than the $\eta\pi^-\pi^0$ channel, interesting candidates are the decay channels $K^-\pi^-K^+$ and $K^-\pi^-\pi^+$. Recently, the corresponding branching ratios have been considered [4] and it appears that the branching ratios alone are not sufficient to determine the presence of the anomaly. In the course of this paper we will show that a detailed study of angular distributions, as defined in [6,7], is well suited to extract the contribution of the anomaly. Our paper is organized as follows.

In Sec. II we introduce the kinematical parameters which are adapted to the present experimental situation where the direction of flight of the τ lepton cannot be reconstructed and only the hadrons are detected. Then we present, following [6,7], the most general angular distribution of the three hadrons in terms of hadronic structure functions. The dependence of the τ polarization is included. By considering adequate moments in Sec. III we show that all of the hadronic structure functions can be measured without reconstructing the τ rest frame. Section IV is devoted to the hadronic model [4] encoded in the structure functions. We present explicit parametrizations of the form factors for the decays into $\eta\pi^-\pi^0$, $K^-\pi^-K^+$, and $K^-\pi^-\pi^+$. The different parameters of the model have been moved to the Appendix.

Finally, numerical results for the hadronic structure functions of the considered channels are presented in Sec. V, proving that an experimental determination of the anomaly is feasible. We anticipate our results and urge experimentalists to analyze the $K^-\pi^-\pi^+$ channel which could contain radial excitations of the K^* which cannot be obtained in e^+e^- experiments.

II. LEPTON TENSOR AND ANGULAR DISTRIBUTION

Let us consider the τ decay

$$\tau(l,s)\to\nu(l',s')+h_1(q_1,m_1)+h_2(q_2,m_2)+h_3(q_3,m_3)\ , \tag{1}$$

where $h_i(q_i,m_i)$ are pseudoscalar mesons. The matrix element reads as

$$\mathcal{M}=\frac{G}{\sqrt{2}}\begin{bmatrix}\cos\theta_C\\ \sin\theta_c\end{bmatrix}M_\mu J^\mu \tag{2}$$

with G the Fermi coupling constant. The cosine and the sine of the Cabibbo angle (θ_C) in (2) have to be used for Cabibbo-allowed $\Delta S=0$ and Cabibbo-suppressed $|\Delta S|=1$ decays, respectively. The leptonic (M_μ) and hadronic (J^μ) currents are given by

$$M_\mu=\bar{u}(l',s')\gamma_\mu(1-\gamma_5)u(l,s) \tag{3}$$

and

$$J^\mu(q_1,q_2,q_3)=\langle h_1(q_1)h_2(q_2)h_3(q_3)|V^\mu(0)-A^\mu(0)|0\rangle\ , \tag{4}$$

where V^μ and A^μ are the vector and axial-vector quark currents, respectively. The most general ansatz for the matrix element of the quark current J^μ in (4) is characterized by four form factors [4,7]:

$$J^\mu(q_1,q_2,q_3)=V_1^\mu F_1+V_2^\mu F_2+iV_3^\mu F_3+V_4^\mu F_4\ , \tag{5}$$

with

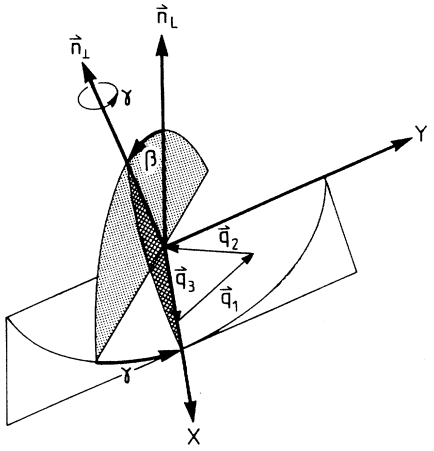

FIG. 1. Definition of the polar angle β and the azimuthal angle γ. β denotes the angle between $\mathbf{n}_\perp$ and $\mathbf{n}_L$. γ denotes the angle between the $(\mathbf{n}_L,\mathbf{n}_\perp)$ plane and the $(\mathbf{n}_\perp,\hat{q}_3)$ plane.

$$
\begin{aligned}
V_1^\mu &= q_1^\mu - q_3^\mu - Q^\mu \frac{Q(q_1-q_3)}{Q^2} , \\
V_2^\mu &= q_2^\mu - q_3^\mu - Q^\mu \frac{Q(q_2-q_3)}{Q^2} , \\
V_3^\mu &= \epsilon^{\mu\alpha\beta\gamma} q_{1\alpha} q_{2\beta} q_{3\gamma} , \\
V_4^\mu &= q_1^\mu + q_2^\mu + q_3^\mu = Q^\mu .
\end{aligned} \tag{6}
$$

The Wess-Zumino anomaly which is of main interest in the present paper gives rise to the term proportional to F_3. The terms proportional to F_1 and F_2 originate from the axial-vector current. Together they correspond to a spin-1 hadronic final state while the F_4 term is due to the spin-0 part of the axial-vector current. As it has been shown in [4], the spin-0 contributions are extremely small and we neglect them in the rest of this paper; i.e., F_4 is set equal to 0.

The differential decay rate is obtained from

$$
d\Gamma(\tau\to\nu_\tau 3h) = \frac{1}{2m_\tau}\frac{G^2}{2}\begin{bmatrix}\cos^2\theta_C \\ \sin^2\theta_C\end{bmatrix}\{L_{\mu\nu}H^{\mu\nu}\}dS^{(4)} , \tag{7}
$$

where $L_{\mu\nu}=M_\mu(M_\nu)^\dagger$ and $H^{\mu\nu}\equiv J^\mu(J^\nu)^\dagger$.

Reaction (1) is most easily analyzed in the hadronic rest frame $\mathbf{q}_1+\mathbf{q}_2+\mathbf{q}_3=0$. The orientation of the hadronic system is characterized by three Euler angles (α,β, and γ) introduced in [6,7]. In current $e^+ + e^-$ [$\to\tau^+\tau^-$ ($\to\nu_\tau 3$ mesons)] experiments, two out of three Euler angles are measurable. The measurable ones are defined by

$$
\begin{aligned}
\cos\beta &= \hat{\mathbf{n}}_L\cdot\hat{\mathbf{n}}_\perp , \\
\cos\gamma &= -\frac{\hat{\mathbf{n}}_L\cdot\hat{\mathbf{q}}_3}{|\hat{\mathbf{n}}_L\times\hat{\mathbf{n}}_\perp|} ,
\end{aligned} \tag{8}
$$

where ($\hat{\mathbf{a}}$ denotes a unit three-vector) $\hat{\mathbf{n}}_L=-\hat{\mathbf{n}}_Q$, with $\hat{\mathbf{n}}_Q$ the direction of the hadrons in the laboratory frame, $\hat{\mathbf{n}}_\perp=\hat{\mathbf{q}}_1\times\hat{\mathbf{q}}_2$, the normal to the plane defined by the momenta of particles 1 and 2. Note that the angle γ defines a rotation around $\hat{\mathbf{n}}_\perp$ and determines the orientation of the three hadrons within their production plane. The definition of the angles β and γ is shown in Fig. 1.

Performing the integration over the unobservable neutrino and the unobservable Euler angle α we obtain the differential decay width for a polarized τ [6,7]:

$$
d\Gamma(\tau\to 3h) = \frac{G^2}{2m_\tau}\begin{bmatrix}\cos^2\theta_C \\ \sin^2\theta_C\end{bmatrix}\left\{\sum_X \bar{L}_X W_X\right\}\frac{1}{(2\pi)^5}\frac{1}{64}\frac{(m_\tau^2-Q^2)^2}{m_\tau^2}\frac{dQ^2}{Q^2}ds_1 ds_2\frac{d\gamma}{2\pi}\frac{d\cos\beta}{2}\frac{d\cos\theta}{2} . \tag{9}
$$

In (9) we have defined the invariant masses in the Dalitz plot $s_i=(q_j+q_k)^2$ (where $i,j,k=1,2,3$; $i\neq j\neq k$) and the square of the invariant mass of the hadron system $Q^2\equiv(q_1+q_2+q_3)^2$. The angle θ is related to the hadronic energy in the laboratory frame E_h by [6–8]

$$
\cos\theta = \frac{2xm_\tau^2 - m_\tau^2 - Q^2}{(m_\tau^2-Q^2)\sqrt{1-4m_\tau^2/s}} , \tag{10}
$$

with

$$
x = 2\frac{E_h}{\sqrt{s}}, \quad s = 4E_{\text{beam}}^2 . \tag{11}
$$

Another quantity depending on this energy E_h is

$$
\cos\psi = \frac{x(m_\tau^2+Q^2)-2Q^2}{(m_\tau^2-Q^2)\sqrt{x^2-4Q^2/s}} , \tag{12}
$$

which will be of some interest in the subsequent discussion. Finally, in the case where the spin-0 part of the hadronic current J^μ is 0 [$F_4=0$ in (5)], $\sum_X \bar{L}_X W_X$ is given by a sum of nine terms $\bar{L}_X W_X$ with $X\in\{A,B,C,D,E,F,G,H,I\}$ corresponding to nine density matrix elements of the hadronic system in a spin-1 state. One has [7]

$$
\begin{aligned}
\bar{L}_A &= \tfrac{2}{3}K_1 + K_2 + \tfrac{1}{3}\overline{K_1}(3\cos^2\beta-1)/2 , \\
\bar{L}_B &= \tfrac{2}{3}K_1 + K_2 - \tfrac{2}{3}\overline{K_1}(3\cos^2\beta-1)/2 , \\
\bar{L}_C &= -\tfrac{1}{2}\overline{K_1}\sin^2\beta\cos 2\gamma , \\
\bar{L}_D &= \tfrac{1}{2}\overline{K_1}\sin^2\beta\sin 2\gamma , \\
\bar{L}_E &= \overline{K_3}\cos\beta , \\
\bar{L}_F &= \tfrac{1}{2}\overline{K_1}\sin 2\beta\cos\gamma , \\
\bar{L}_G &= -\overline{K_3}\sin\beta\sin\gamma , \\
\bar{L}_H &= -\tfrac{1}{2}\overline{K_1}\sin 2\beta\sin\gamma , \\
\bar{L}_I &= -\overline{K_3}\sin\beta\cos\gamma ,
\end{aligned} \tag{13}
$$

where

$$
\begin{aligned}
K_1 &= 1 - P\cos\theta - (m_\tau^2/Q^2)(1+P\cos\theta)\ , \\
K_2 &= (m_\tau^2/Q^2)(1+P\cos\theta)\ , \\
K_3 &= 1 - P\cos\theta\ , \\
\overline{K_1} &= K_1(3\cos^2\psi - 1)/2 - \tfrac{3}{2}K_4\sin 2\psi\ , \\
\overline{K_2} &= K_2\cos\psi + K_4\sin\psi\ , \\
\overline{K_3} &= K_3\cos\psi - K_5\sin\psi\ , \\
K_4 &= \sqrt{m_\tau^2/Q^2}\,P\sin\theta\ , \\
K_5 &= \sqrt{m_\tau^2/Q^2}\,P\sin\theta\ .
\end{aligned}
\tag{14}
$$

In (14), P denotes the polarization of the τ in the laboratory frame while θ and ψ are defined in Eqs. (10) and (12). For physics of the CERN e^+e^- collider LEP (Z decay) P is given by $P=-2v_\tau a_\tau/(v_\tau^2+a_\tau^2)$, with $v_\tau=-1+4\sin^2\theta_W$ and $a_\tau=-1$, while for lower energies P vanishes. In this case (for ARGUS, CLEO) Eq. (14) simplifies to

$$
\begin{aligned}
K_1 &= 1 - m_\tau^2/Q^2 = \frac{2\overline{K_1}}{3\cos^2\psi - 1}\ , \\
K_2 &= m_\tau^2/Q^2 = \frac{\overline{K_2}}{\cos\psi}\ , \\
K_3 &= 1 = \frac{\overline{K_3}}{\cos\psi}\ .
\end{aligned}
\tag{15}
$$

Note that the *full* dependence on the τ polarization P, the hadron energy (through θ and ψ), and the angles β and γ are given in Eqs. (13)–(15).

The hadronic functions W_X contain the dynamics of the hadronic decay and depend in general on s_1, s_2, and Q^2. Let us recall that we are working in the hadronic rest frame with the z and x axes aligned along $\hat{\mathbf{n}}_\perp$ and $\hat{\mathbf{q}}_3$, respectively (see Fig. 1). The hadronic tensor $H^{\mu\nu}=J^\mu(J^\nu)^\dagger$ [with J^μ given in (5)] is calculated in this frame and the hadronic structure functions W_X are linear combinations of density matrix elements which are obtained from

$$
H^{\sigma\sigma'} = \epsilon_\mu(\sigma) H^{\mu\nu} \epsilon_\nu^*(\sigma')\ ,
\tag{16}
$$

where

$$
\epsilon_\mu(\pm) = \frac{1}{\sqrt{2}}(0;\pm 1,-i,0),\quad \epsilon_\mu(0) = (0;0,0,1)
\tag{17}
$$

are the polarization vectors for a hadronic system in a spin-1 state defined with respect to the normal on the three meson plane in the hadronic rest frame. The pure spin-1 structure functions are

$$
\begin{aligned}
W_A &= H^{++} + H^{--} = H^{11} + H^{22}\ , \\
W_B &= H^{00} = H^{33}\ , \\
W_C &= -(H^{+-} + H^{-+}) = H^{11} - H^{22}\ , \\
W_D &= i(H^{+-} - H^{-+}) = H^{12} + H^{21}\ , \\
W_E &= H^{++} - H^{--} = -i(H^{12} - H^{21})\ , \\
W_F &= -(H^{+0} + H^{0+} - H^{-0} - H^{0-})/\sqrt{2} = H^{13} + H^{31}\ , \\
W_G &= i(H^{+0} - H^{0+} - H^{-0} + H^{0-})/\sqrt{2} = -i(H^{13} - H^{31})\ , \\
W_H &= i(H^{+0} - H^{0+} + H^{-0} - H^{0-})/\sqrt{2} = H^{23} + H^{32}\ , \\
W_I &= (H^{+0} + H^{0+} + H^{-0} + H^{0-})/\sqrt{2} = -i(H^{23} - H^{32})\ .
\end{aligned}
\tag{18}
$$

The right-hand sides of Eqs. (18) refer to the Cartesian components of $H^{\mu\nu}$. The structure functions can thus be expressed in terms of the form factors F_i as [7]

$$
\begin{aligned}
W_A &= (x_1^2 + x_3^2)|F_1|^2 + (x_2^2 + x_3^2)|F_2|^2 + 2(x_1x_2 - x_3^2)\mathrm{Re}(F_1F_2^*)\ , \\
W_B &= x_4^2|F_3|^2\ , \\
W_C &= (x_1^2 - x_3^2)|F_1|^2 + (x_2^2 - x_3^2)|F_2|^2 + 2(x_1x_2 + x_3^2)\mathrm{Re}(F_1F_2^*)\ , \\
W_D &= 2[x_1x_3|F_1|^2 - x_2x_3|F_2|^2 + x_3(x_2 - x_1)\mathrm{Re}(F_1F_2^*)]\ , \\
W_E &= -2x_3(x_1 + x_2)\mathrm{Im}(F_1F_2^*)\ , \\
W_F &= 2x_4[x_1\mathrm{Im}(F_1F_3^*) + x_2\mathrm{Im}(F_2F_3^*)]\ , \\
W_G &= -2x_4[x_1\mathrm{Re}(F_1F_3^*) + x_2\mathrm{Re}(F_2F_3^*)]\ , \\
W_H &= 2x_3x_4[\mathrm{Im}(F_1F_3^*) - \mathrm{Im}(F_2F_3^*)]\ , \\
W_I &= -2x_3x_4[\mathrm{Re}(F_1F_3^*) - \mathrm{Re}(F_2F_3^*)]\ ,
\end{aligned}
\tag{19}
$$

where x_i are functions of the Dalitz plot variables and Q^2. One has

$$
\begin{aligned}
x_1 &= q_1^x - q_3^x\ , \\
x_2 &= q_2^x - q_3^x\ , \\
x_3 &= q_1^y = -q_2^y\ , \\
x_4 &= \sqrt{Q^2}\,x_3 q_3^x\ .
\end{aligned}
\tag{20}
$$

Here E_i and q_i refers to the components of the hadron momenta in the hadronic rest frame with

$$\begin{aligned} E_i &= \frac{Q^2 - s_i + m_i^2}{2\sqrt{Q^2}} , \\ q_3^x &= \sqrt{E_3^2 - m_3^2} , \\ q_2^x &= (2E_2E_3 - s_1 + m_2^2 + m_3^2)/(2q_3^x) , \\ q_1^x &= (2E_1E_3 - s_2 + m_1^2 + m_3^2)/(2q_3^x) , \\ q_2^y &= -\sqrt{E_2^2 - (q_2^x)^2 - m_2^2} , \\ q_1^y &= \sqrt{E_1^2 - (q_1^x)^2 - m_1^2} = -q_2^y . \end{aligned} \tag{21}$$

Note that the structure functions $W_{B,F,G,H,I}$ are related to the anomaly form factor F_3. In the following we will consider these structure functions in more detail.

III. DEFINITION OF MOMENTS

Equation (9) provides the full description of the angular distribution of the decay products from a single polarized τ. They reveal that the measurement of the structure functions W_i, and therefore the measurements of the anomaly form factor F_3, is possible in currently ongoing high statistics experiments. In the following we will concentrate on the s_1, s_2 integrated structure functions:

$$w_i(Q^2) \equiv \int ds_1 ds_2 W_i(Q^2, s_1, s_2) . \tag{22}$$

A possible strategy to isolate the various structure functions in (9) is to take suitable moments on the differential decay distribution [7]. Let us define[1]

$$\langle f(\beta,\gamma) \rangle_R = \int \frac{8\pi\sqrt{Q^2} d\Gamma(\tau \to \nu_\tau 3h)}{dQ^2 d\cos\theta \, d\gamma \, d\cos\beta} f(\beta,\gamma) \frac{d\cos\beta}{2} \frac{d\gamma}{2\pi} , \tag{23}$$

which yields

$$\begin{aligned} \langle 1 \rangle_R &= R_c^s(Q^2)(2K_1 + 3K_2)(w_A + w_B) , \\ \langle (3\cos^2\beta - 1)/2 \rangle_R &= R_c^s(Q^2) \tfrac{1}{5} \overline{K_1} (w_A - 2w_B) , \\ \langle \cos 2\gamma \rangle_R &= -R_c^s(Q^2) \tfrac{1}{2} \overline{K_1} w_C , \\ \langle \sin 2\gamma \rangle_R &= R_c^s(Q^2) \tfrac{1}{2} \overline{K_1} w_D , \\ \langle \cos\beta \rangle_R &= R_c^s(Q^2) \overline{K_3} w_E , \\ \langle \sin 2\beta \cos\gamma \rangle_R &= R_c^s \tfrac{2}{5} \overline{K_1} w_F , \\ \langle \sin\beta \sin\gamma \rangle_R &= -R_c^s(Q^2) \overline{K_3} w_G , \\ \langle \sin 2\beta \sin\gamma \rangle_R &= -R_c^s(Q^2) \tfrac{2}{5} \overline{K_1} w_H , \\ \langle \sin\beta \cos\gamma \rangle_R &= -R_c^s(Q^2) \overline{K_3} w_I , \end{aligned} \tag{24}$$

where the function $R_c^s(Q^2)$ has been defined by

$$R_c^s(Q^2) = \frac{G^2}{12 m_\tau^3} \begin{bmatrix} \cos^2\theta_C \\ \sin^2\theta_C \end{bmatrix} \frac{1}{(4\pi)^5} \frac{(m_\tau^2 - Q^2)^2}{\sqrt{Q^2}} . \tag{25}$$

Some comments are in order here.

First note that after integration over the angles β and γ the preceding expressions are still dependent on P and E_h (through θ and ψ), while the hadronic structure functions w_X are functions of Q^2.

The sum $w_A + w_B$ is closely related to the spin-1 part of the spectral function

$$\rho_1(Q^2) = \frac{1}{6} \frac{1}{(4\pi)^4} \frac{1}{Q^4} (w_A + w_B) \tag{26}$$

and we obtain the standard form for the total width

$$\begin{aligned} \Gamma(\tau \to \nu_\tau 3h) &= \frac{G^2}{8\pi m_\tau} \begin{bmatrix} \cos^2\theta_C \\ \sin^2\theta_C \end{bmatrix} \int dQ^2 (m_\tau^2 - Q^2)^2 \left[1 + \frac{2Q^2}{m_\tau^2} \right] \rho_1(Q^2) \\ &= \int \frac{dQ^2}{\sqrt{Q^2}} R_c^s(Q^2) \left[\frac{m_\tau^2 + 2Q^2}{Q^2} \right] (w_A + w_B) . \end{aligned} \tag{27}$$

In our figures in Sec. V we will present the functions $R_c^s(Q^2) w_X(Q^2)$ as well as numerical results for the hadronic structure functions $w_X(Q^2)$ itself.

In the next section we present an explicit parametrization of the form factors which are used in our numerical simulations in order to test whether the anomaly can be measured experimentally.

IV. FORM FACTORS

In a recent paper [4] we have given an explicit parametrization of the form factors and compared them successfully with measured widths. The physical idea behind the model for the form factors can be resummed to the following.

[1]Note that these moments differ from the moments defined in (7) by the factor R_c^s defined in (25).

In the chiral limit the form factors are normalized to the $U(3)_L \times U(3)_R$ chiral model.

Meson-vertices are independent of momentum.

The full momentum dependence is given by Breit-Wigner propagators of the resonances occurring in the different channels. Resonances occur either in Q^2, which are then three-body resonances, or in s_i which are two-body resonances. Now we present our parametrization for the form factors F_i defined in (5) which fulfill all these requirements.

First we present the form factors induced by the anomaly

$$F_3^{(\eta\pi^-\pi^0)}(s_1,Q^2)=\frac{1}{2\sqrt{6}\pi^2 f_\pi^3}T_\rho^{(2)}[Q^2]T_\rho^{(1)}[s_1]\ , \tag{28}$$

$$F_3^{(K^-\pi^-K^+)}(s_1,s_2,Q^2)=\frac{-1}{2\sqrt{2}\pi^2 f_\pi^3}T_\rho^{(2)}[Q^2]T_{\rho K^*}(s_2,s_1,\alpha)\ , \tag{29}$$

$$F_3^{(K^-\pi^-\pi^+)}(s_1,s_2,Q^2)=\frac{1}{2\sqrt{2}\pi^2 f_\pi^3}T_{K^*}^{(1,2)}[Q^2]T_{\rho K^*}(s_1,s_2,\alpha)\ . \tag{30}$$

The parametrization of the $\eta\pi^-\pi^0$ channel is obtained from $e^+ + e^-$ data via CVC [3,4]. It is given as a product of two functions describing the resonances in Q^2 and s_i. The same Q^2 dependence ($T_p^{(2)}[Q^2]$) can be used for the $K^-\pi^-K^+$ channel. Of course, the two-body channels have to be modified since they involve a ρ and a K^* as well; we have included these contributions in $T_{\rho K^*}(s_2,s_1,\alpha)$ [4]. The same function $T_{\rho K^*}$ also enters in the $K^-\pi^-\pi^+$ channel. Unfortunately, nothing is known experimentally on the three-body resonances in this channel. In [4] only the K^* resonance ($T_{K^*}^{(1)}$) has been included. In our numerical results we will also use a different parametrization including more $\Delta S=1$ vector resonances.

Second, the axial-vector current induces two form factors F_1 and F_2 for the $K^-\pi^-K^+$ and $K^-\pi^-\pi^+$ channels with the parametrization

$$F_1^{(K^-\pi^-K^+)}(s_2,Q^2)=\frac{-\sqrt{2}}{3f_\pi}P_{A_1}^{\mathrm{BW}}[Q^2]T_\rho^{(1)}[s_2]\ , \tag{31}$$

$$F_2^{(K^-\pi^-K^+)}(s_1,Q^2)=\frac{-\sqrt{2}}{3f_\pi}P_{A_1}^{\mathrm{BW}}[Q^2]T_{K^*}^{(1)}[s_1]\ , \tag{32}$$

and

$$F_1^{(K^-\pi^-\pi^+)}(s_2,Q^2)=\frac{-\sqrt{2}}{3f_\pi}P_{K_1}^{\widehat{\mathrm{BW}}}[Q^2]T_{K^*}^{(1)}[s_2]\ , \tag{33}$$

$$F_2^{(K^-\pi^-\pi^+)}(s_1,Q^2)=\frac{-\sqrt{2}}{3f_\pi}P_{K_1}^{\widehat{\mathrm{BW}}}[Q^2]T_\rho^{(1)}[s_1]\ . \tag{34}$$

Note that G parity forbids the axial-vector current to contribute to the $\eta\pi^-\pi^0$ channel. In the axial-vector channel we assume the dominance of a resonance in each channel, i.e., the A_1 and the K_1 in the $\Delta S=0$ and $\Delta S=1$ channels, respectively. The two-body channels are again parametrized by the functions $T_\rho^{(1)}$ and $T_{K^*}^{(1)}$. We have moved explicit expressions of these functions and all numerical parameters (taken from [4]) to the Appendix.

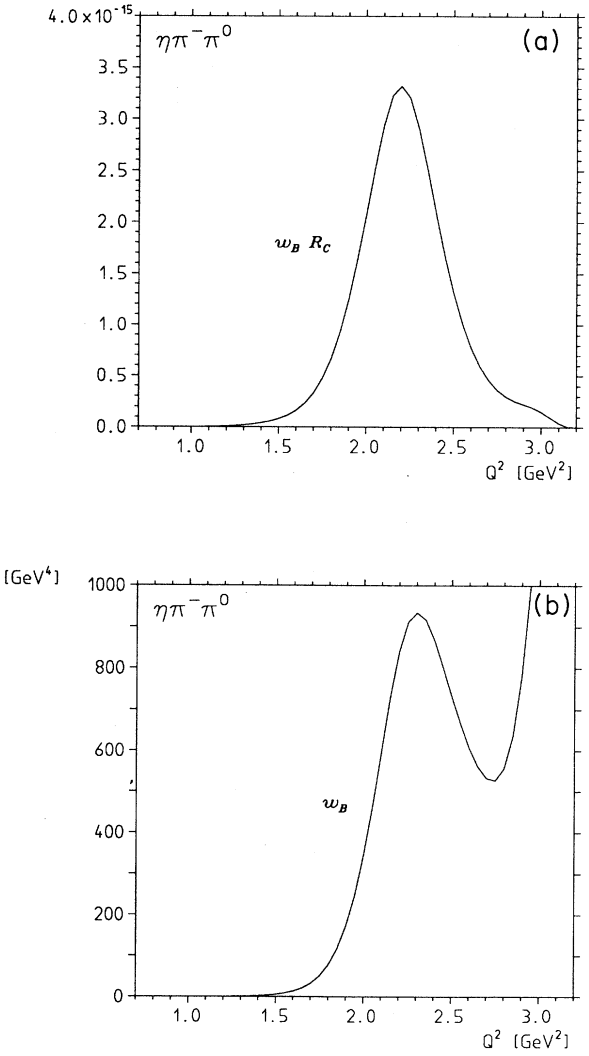

FIG. 2. (a) Q^2 dependence of $w_B \cdot R_C$ for the decay channel $\eta\pi^-\pi^0$. (b) Q^2 dependence of w_B for the decay channel $\eta\pi^-\pi^0$.

V. NUMERICAL RESULTS

In this section we will present numerical results for $R_c(Q^2)w_X(Q^2)$ [defined in (22) and (25)] as well as for the hadronic structure functions $w_X(Q^2)$ separately for the different decay channels. We prefer to present both $R_c w_X$ and w_X in order to show the effect of the phase space (included in the function R_c) while the hadronic physics is more visible in the plots for w_X alone. Although by integrating over s_1 and s_2 we have lost information on the resonances in the two-body decays we observe still interesting structures.

Let us start with the Cabibbo-allowed decay $\tau \to \nu_\tau + \eta\pi^-\pi^0$. As mentioned before, this channel has a vanishing contribution from the axial-vector current (G parity) which implies that only w_B is different from zero. A comparison of the data and our prediction for $R_C\, w_B$ and w_B in Figs. 2(a) and 2(b) would be highly interesting, especially as a confirmation of higher-lying ρ resonances in $T_\rho^{(2)}(Q^2)$ [the shoulder at $Q^2=3$ GeV^2 in Figs. 2(a) and 2(b)].

The next process is the Cabibbo-allowed decay $\tau \to \nu_\tau K^-\pi^-K^+$ which has contributions from both the axial-vector and vector currents. Therefore all nine structure functions are different from zero. In Fig. 3(a) we present the structure function combinations obtained from the $\langle 1 \rangle_R$ and $\langle (3\cos^2\beta - 1)/2) \rangle_R$ moment. Note that a measurement of the differential decay width (proportional to $\langle 1 \rangle_R$) is not enough to separate w_A and w_B. We observe a sizable effect of w_B which makes a determination of F_3 possible. Note this sizable effect is due to heavy ρ' resonances in the anomaly channel, the existence

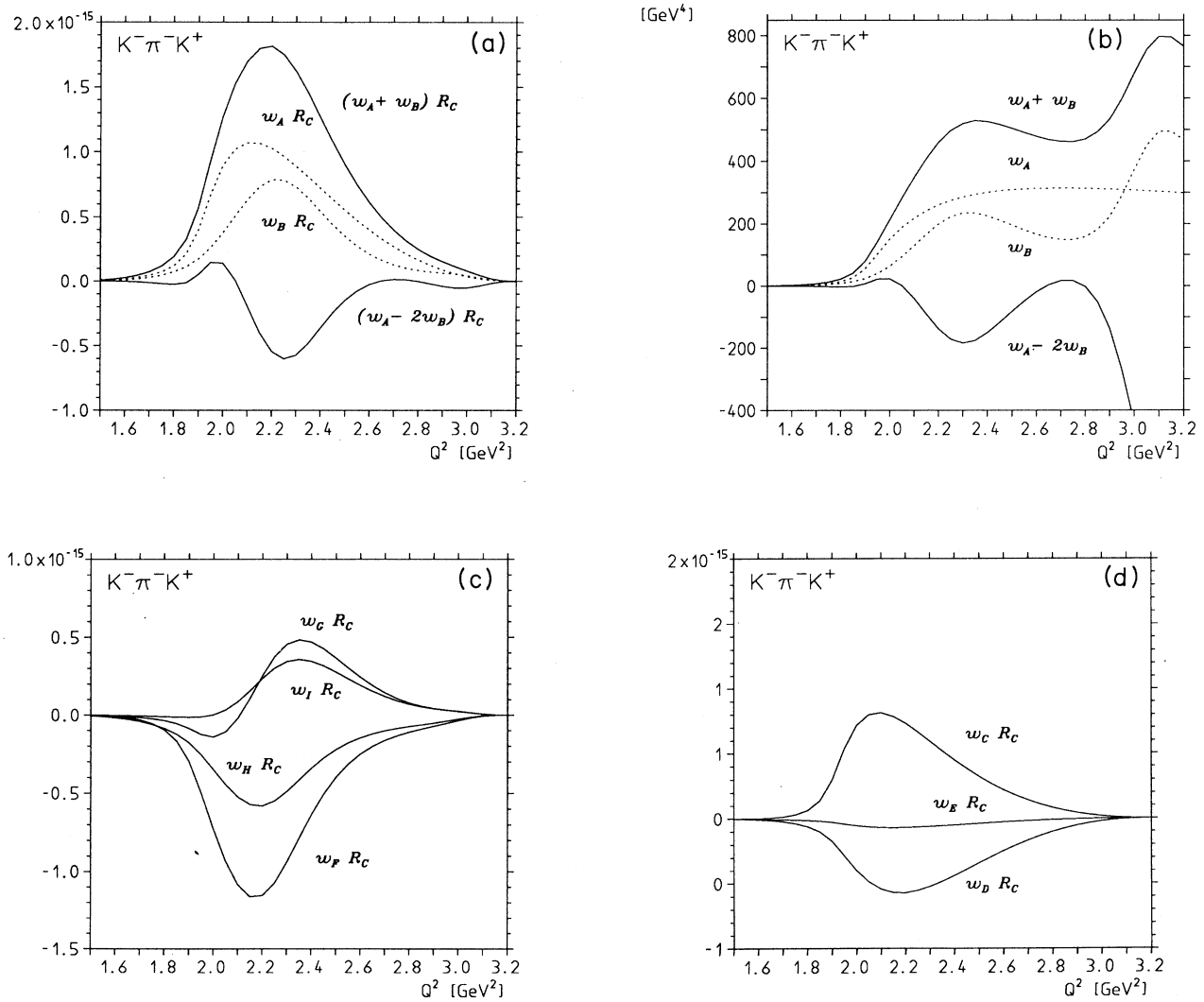

FIG. 3. (a) Q^2 dependence of $(w_A+w_B)\cdot R_C$, $(w_A-2w_B)\cdot R_C$, $w_A\cdot R_C$, and $w_B\cdot R_C$ for the decay channel $K^-\pi^-K^+$. (b) Q^2 dependence of (w_A+w_B), (w_A-2w_B), w_A, and w_B for the decay channel $K^-\pi^-K^+$. (c) Q^2 dependence of $w_F\cdot R_C$, $w_G\cdot R_C$, $w_H\cdot R_C$, and $w_I\cdot R_C$ for the decay channel $K^-\pi^-K^+$. (d) Q^2 dependence of $w_C\cdot R_C$, $w_D\cdot R_C$, and $w_E\cdot R_C$ for the decay channel $K^-\pi^-K^+$.

of which is predicted from the description of $e^+e^- \to \eta\pi\pi$. In order to get a feeling of the effects of the phase space in this channel we present the combinations $w_A + w_B$ and $w_A - 2w_B$, as well as the structure functions w_A and w_B in Fig. 3(b). The moments which measure the interference of the axial-vector and vector currents are presented in Fig. 3(c). The size of these moments is comparable to those in Fig. 3(a), and the very peculiar shape would make them measurable too. For completeness we present the remaining moments in Fig. 3(d).

Finally we discuss the Cabibbo-suppressed decay $\tau \to \nu_\tau K^- \pi^- \pi^+$ in Figs. 4(a)–4(d) for the parametrization with $T^{(1)}_{K^*}$ in (30). Note that although this decay is Cabibbo suppressed, the moments are comparable in size to the $K^-\pi^+K^+$ case (suppression due to the mass of the supplementary kaon in the phase space is comparable to the Cabibbo suppression). All moments of Figs. 4(a)–4(d) have a shape which shows the strong presence of the K_1 resonance in the axial channel. A measurement of the structure functions related to the anomaly seems very hard since F_3 is very small in this parametrization. Of course this unfavorable result could have been deduced since the contribution of the anomaly to the rate, as computed in [4], was of the order of 1%. However, we should note that our parametrization of the anomaly form factor [4] includes only a K^*, which can never be on mass shell, and therefore produces no strong enhancement. On the other hand, in this channel we have no CVC prediction which could tell us if heavier resonances are present in this channel. In order to get a feeling for possible effects of heavier K^* resonances we propose the following parametrization which is ρ-channel inspired [see Eq. (A6)]:

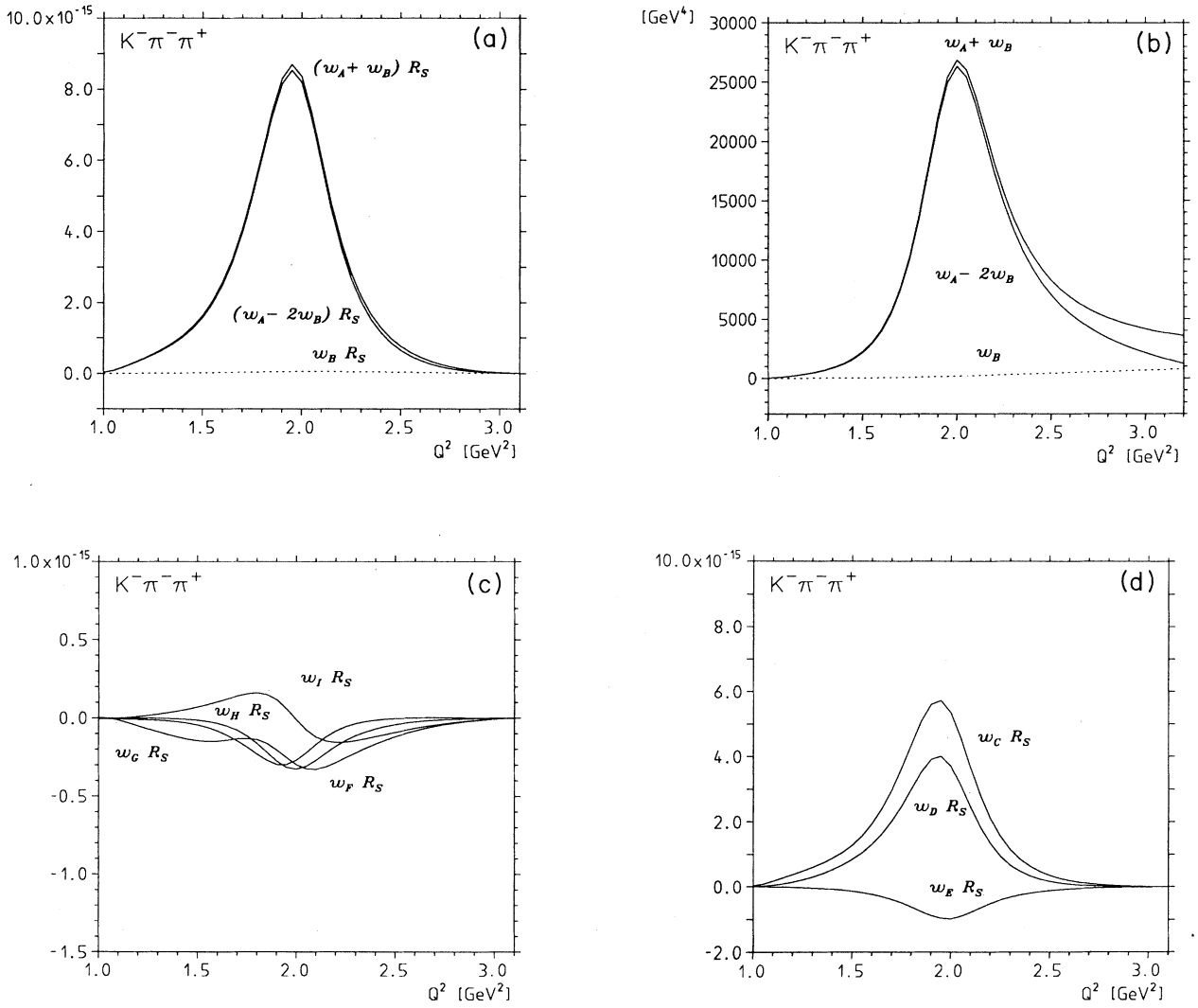

FIG. 4. (a) Q^2 dependence of $(w_A + w_B)\cdot R_S$, $(w_A - 2w_B)\cdot R_S$, and $w_B \cdot R_S$ for the decay channel $K^-\pi^-\pi^+$ with the parametrization $T^{(1)}_{K^*}$ in (42). (b) Q^2 dependence of $(w_A + w_B)$, $(w_A - 2w_B)$, and w_B for the decay channel $K^-\pi^-\pi^+$ with the parametrization $T^{(1)}_{K^*}$ in (42). (c) Q^2 dependence of $w_F \cdot R_S$, $w_G \cdot R_S$, $w_H \cdot R_S$, and $w_I \cdot R_S$ for the decay channel $K^-\pi^-\pi^+$ with the parametrization $T^{(1)}_{K^*}$ in (A7). (d) Q^2 dependence of $w_S \cdot R_S$, $w_D \cdot R_S$, and $w_E \cdot R_E$ for the decay channel $K^-\pi^-\pi^+$ with the parametrization $T^{(1)}_{K^*}$ in (A7).

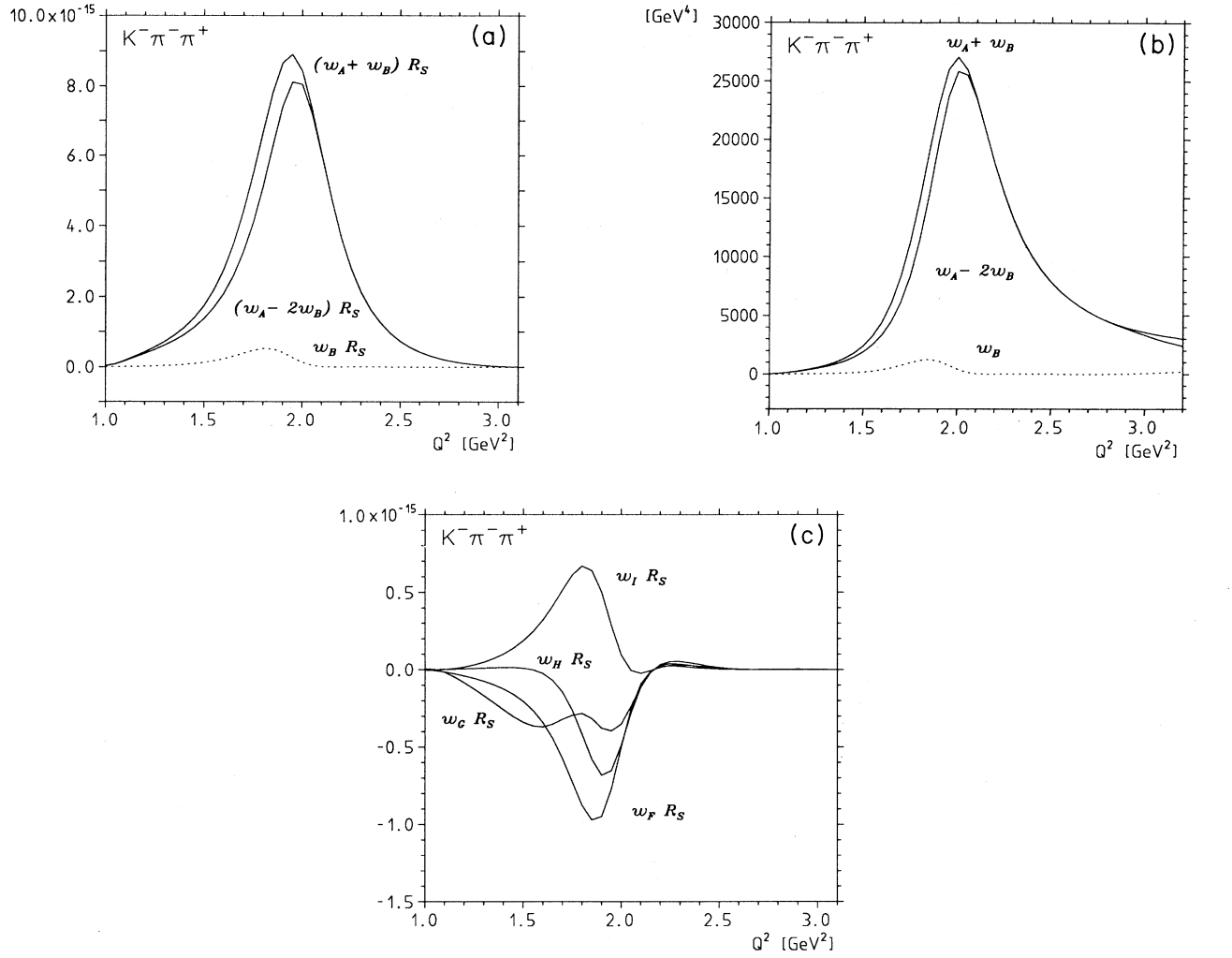

FIG. 5. (a)–(c) same as Fig. 4 with the parametrization $T^{(2)}_{K^*}$ in (35).

$$T^{(2)}_{K^*}[s]=\frac{1}{1+\beta+\delta}\left\{P^{\mathrm{BW}}_{K^*(1680)}[s]+\beta P^{\mathrm{BW}}_{K^*(1410)}[s]+\delta P^{\mathrm{BW}}_{K^*}[s]\right\},$$

$$\delta=-26,\quad m_{K^*}=0.892\ \mathrm{GeV},\quad \Gamma_{K^*}=0.050\ \mathrm{GeV}, \tag{35}$$

$$\beta=6.5,\quad m_{K^*(1410)}=1.412\ \mathrm{GeV},\quad \Gamma_{K^*(1410)}=0.227\ \mathrm{GeV},\quad m_{K^*(1680)}=1.714\ \mathrm{GeV},\quad \Gamma_{K^*(1680)}=0.323\ \mathrm{GeV}.$$

With this parametrization we obtain the results in Figs. 5(a)–5(c). Note that Fig. 4(d) is not changed.

For completeness we present the results of the total decay width $\Gamma^{\eta\pi^-\pi^0}$, $\Gamma^{K^-\pi^-K^+}$, and $\Gamma^{(K^-\pi^-\pi^+)}$ normalized to the electronic width Γ_e ($\Gamma_e/\Gamma_{\mathrm{tot}}\approx 18\%$). One has

Channel (abc)	$\frac{\Gamma^{(abc)}}{\Gamma_e}$	Contribution from F_3 in %
$\eta\pi^-\pi^0$	0.0108	100%
$K^-\pi^-K^+$	0.0061	39.3%
$K^-\pi^-\pi^+$	0.0316	1.1% with $T^{(1)}_{K^*}$
$K^-\pi^-\pi^+$	0.0325	4.2% with $T^{(2)}_{K^*}$

In view of this result we urge our experimental colleagues to study carefully this Cabibbo-suppressed channel.

VI. CONCLUSIONS

In this paper we have proposed to measure moments [Eq. (23)] which allows us to determine quantitatively the contribution of the Wess-Zumino anomaly to τ decays into three mesons. We have considered the channels $\eta\pi^-\pi^0$, $K^-\pi^-K^+$, and $K^-\pi^-\pi^+$. We have shown that measuring the unique moment of the $\eta\pi^-\pi^0$ channel al-

lows us to verify the CVC prediction, especially the presence of heavy ρ excitations observed in $e^+ + e^-$ data [9]. In the $K^-\pi^-K^+$ channel we can define many more moments because of the interference of the anomaly with the axial-vector contributions. In our prediction (Fig. 3) the effect of the heavier ρ is again clearly seen.

The interest of the analysis of the $K^-\pi^-\pi^+$ is twofold: we learn something about resonances, first in the axial-vector channel and second in the vector channel. We noted that in contradistinction to the Cabibbo-allowed decays the vector channel for Cabibbo-suppressed decays cannot be predicted through CVC from $e^+ + e^-$ data.

APPENDIX: PARAMETERS USED IN THE FORM FACTORS

As stated in Sec. IV the form factors are dominated by resonances. The effects of these resonances are described by functions $P_P^{\mathrm{BW}}(Q^2)$, which are normalized $[P_P^{\mathrm{BW}}(0)=1]$ Breit-Wigner propagators. We will use two kinds of Breit-Wigner propagators.

(i) Energy-dependent width:

$$P_R^{\mathrm{BW}}[s]\equiv\frac{-M_R^2}{s-M_R^2+i\sqrt{s}\,\Gamma_R(s)}\ . \tag{A1}$$

The energy-dependent width $[\Gamma_R(s)]$ is computed from its usual definition:

$$\Gamma_R(s)=\frac{1}{2\sqrt{s}}|M_{R\to f_1}|^2 d\Phi\,\delta\left[Q-\sum p_i\right],\quad \Gamma_R(s)_{s=M_R^2}=\Gamma_R\ . \tag{A2}$$

(ii) Constant width:

$$P_R^{\hat{\mathrm{BW}}}[s]\equiv\frac{-M_R^2+iM_R\Gamma_R}{s-M_R^2+iM_R\Gamma_R}\ . \tag{A3}$$

First we define the parameters which arise in the axial-vector three-body channel: In the Breit-Wigner propagator of the A_1 we use

$$m_{A_1}=1.251\ \mathrm{GeV},\quad \Gamma_{A_1}=0.599\ \mathrm{GeV},\quad \sqrt{s}\,\Gamma_{A_1}(s)=m_{A_1}\Gamma_{A_1}\frac{g(s)}{g(m_{A_1}^2)}\ , \tag{A4}$$

where the function $g(s)$ has been calculated in [10]:

$$g(s)=\begin{cases}4.1(s-9m_\pi^2)^3[1-3.3(s-9m_\pi^2)+5.8(s-9m_\pi^2)^2], & \text{if } s<(m_\rho+m_\pi)^2\ ,\\ s\left[1.623+\dfrac{10.38}{s}-\dfrac{9.32}{s^2}+\dfrac{0.64}{s^2}\right], & \text{otherwise}\ .\end{cases} \tag{A5}$$

In this equation all masses and $\sqrt{s}$ are expressed in GeV.

In the case of the K_1 resonance we use a constant width Breit-Wigner propagator $P_{K_1}^{\hat{\mathrm{BW}}}[s]$ with

$$m_{K_1}=1.402\ \mathrm{GeV},\quad \Gamma_{K_1}=0.174\ \mathrm{GeV}\ .$$

This is because the decay of the K_1 is experimentally not well known.

The Cabibbo-allowed vector form factor is obtained from CVC and yields [9]

$$T_\rho^{(2)}[s]=\frac{1}{1+\beta+\delta}\left\{P_{\rho''}^{\mathrm{BW}}[s]+\beta P_{\rho'}^{\mathrm{BW}}[s]+\delta P_\rho^{\mathrm{BW}}[s]\right\}, \tag{A6}$$

$$\delta=-26,\quad m_\rho=0.773\ \mathrm{GeV},\quad \Gamma_\rho=0.145\ \mathrm{GeV}\ ,$$

$$\beta=6.5,\quad m_{\rho'}=1.500\ \mathrm{GeV},\quad \Gamma_{\rho'}=0.220\ \mathrm{GeV},\quad m_{\rho''}=1.750\ \mathrm{GeV},\quad \Gamma_{\rho''}=0.120\ \mathrm{GeV}\ .$$

For its $\Delta S=1$ we propose (no experimental data) either

$$T_{K^*}^{(1)}[s]\equiv P_{K^*}^{\mathrm{BW}}[s],\quad m_{K^*}=0.892\ \mathrm{GeV},\quad \Gamma_{K^*}=0.051\ \mathrm{GeV}\ , \tag{A7}$$

or the function $T_{K^*}^{(2)}[s]$ defined in (35).

Finally we define the functions describing the resonances in the two-body channel [10]:

$$T_\rho^{(1)}[s]=\frac{1}{1+\beta}\left\{P_\rho^{\mathrm{BW}}[s]+\beta P_{\rho'}^{\mathrm{BW}}[s]\right\}, \quad m_\rho=0.773 \text{ GeV}, \quad \Gamma_\rho=0.145 \text{ GeV},$$

$$\beta=-0.145, \quad m_{\rho'}=1.370 \text{ GeV}, \quad \Gamma_{\rho'}=0.510 \text{ GeV}. \tag{A8}$$

The function $T_{K^*}^{(1)}[s]$ has been defined in (A7). Last but not least we define the function which enters the anomaly two-body channel:

$$T_{\rho K^*}(s_1,s_2,\alpha)=\frac{T_\rho^{(1)}[s_1]+\alpha T_{K^*}[s_2]}{1+\alpha}, \tag{A9}$$

where $T_\rho^{(1)}$ is given in (A8) and $\alpha=-0.2$ [4].

[1] J. Wess and B. Zumino, Phys. Lett. **37B**, 95 (1971).
[2] G. Kramer, W. F. Palmer, and S. Pinsky, Phys. Rev. D **30**, 89 (1984); G. Kramer and W. F. Palmer, Z. Phys. C **25**, 195 (1984); **39**, 423 (1988).
[3] A. Pich, Phys. Lett. B **196**, 561 (1987); F. J. Gilman, Phys. Rev. D **35**, 3541 (1987).
[4] R. Decker, E. Mirkes, R. Sauer, and Z. Was, Z. Phys. C (to be published).
[5] M. Artuso *et al.*, Phys. Rev. Lett. **69**, 3278 (1992).
[6] J. H. Kühn and E. Mirkes, Phys. Lett. B **286**, 381 (1992).
[7] J. H. Kühn and E. Mirkes, Z. Phys. C **56**, 661 (1992).
[8] J. H. Kühn and F. Wagner, Nucl. Phys. **B236**, 16 (1984).
[9] DM2 Collaboration, A. Antonelli *et al.*, Phys. Lett. B **212**, 133 (1988); J. J. Gomez-Cadenas, M. C. Gonzales-Garcia, and A. Pich, Phys. Rev. D **42**, 3093 (1990).
[10] J. H. Kühn and A. Santamaria, Z. Phys. C **48**, 445 (1990).